SCANNING VOL. 24, 264–269 (2002)

Received: February 13, 2002
Accepted: April 8, 2002

Monte Carlo Analysis of the Detection of Clay Occlusion of Respirable Quartz Particles Using Multiple Voltage Scanning Electron Microscopy

V. HNIZDO AND W. E. WALLACE

National Institute for Occupational Safety and Health, Morgantown, West Virginia, USA

Summary: The electron incident-energy dependence of the relative intensities of Al and Si x-rays produced in a respirable-sized quartz particle by scanning electron microscopy is sensitive to the inhomogeneity of the distribution of Al and Si in the particle. Realistic Monte Carlo calculations of this energy dependence validate the proposal to use this effect for the detection of particles in which an aluminosilicate coating occludes the surface of a silica core.

Key words: Monte Carlo, scanning electron microscopy, x-ray microanalysis, respirable quartz, surface coating

PACS: 61.16.Bg

Introduction

Respirable quartz dust is a known cause of pulmonary disease (National Institute for Occupational Safety and Health 1974). However, studies have shown that the quartz content of respirable dust alone is not a reliable predictor of the prevalence of dust-induced disease (LeBouffant *et al.* 1982, Rokbok and Klosterkotter 1973), which suggests that it is the biologically available quartz surface rather than the bulk quartz concentration that is more relevant in this context. Scanning electron microscopy (SEM) x-ray spectrometry is a valuable tool for determining the elemental composition of individual dust particles, but the conventional SEM x-ray analysis does not yield information on the possible inhomogeneity of the distribution of any given element in a particle. Electron microprobe microanalysis using different incident electron accelerating voltages has been used to analyze thin metallic surface coatings on other metal substrates (Pouchou and Pichoir 1984). Wallace *et al.* (1990) have proposed to use the dependence of the x-ray yields on the incident electron energy as a probe of the heterogeneity of a particle's structure. To this end, they developed a simple one-dimensional model of x-ray production and absorption in a multilayered medium, and using this model they were able to demonstrate the feasibility of the detection of a thin aluminosilicate coating on a silica core in a respirable dust particle by the measurement of the energy dependence of the ratio Si to Si+Al x-ray yields at low energies (~5 keV) of the incident electrons.

It is desirable to develop further the analytical model of Wallace *et al.* with a view to obtaining a quantitatively accurate method of analysis of the structure heterogeneity in respirable particles. The Monte Carlo method has become an invaluable computational tool of analysis in SEM work since its first applications to this field in the mid 1970s (Heinrich *et al.* 1976). The Monte Carlo method is well suited to a realistic modeling of the electron-scattering and x-ray-production stochastic processes in a finite three-dimensional medium of a given shape and heterogeneous composition, which is a task that is generally intractable in a traditional analytical treatment.

In this paper, we present the results of realistic Monte Carlo calculations of the production of x-rays by low-energy (5–30 keV) electrons incident on a spherical particle of respirable size (~1 μm), whose core is coated with a layer of a different composition than that of the core. These calculations furnish the ratio of the Si to Si+Al x-ray yields as a function of the incident electron energy for a range of thicknesses of aluminosilicate surface layers and silica core radii. We shall describe first the Monte Carlo model used. The Results and Discussion section contains the presentation of the calculational results, their comparison with experimental data, and a discussion. The Conclusion is drawn in the last section.

The Monte Carlo Model

We used the Monte Carlo method of the simulation of electron scattering and x-ray production (see, e.g., Joy 1995, Newbury *et al.* 1986) to model the physical processes of our interest as follows.

Electron Scattering

A narrow beam of electrons of an energy in the range 5–30 keV is incident on the surface a spherical particle,

Address for reprints:

Vladimir Hnizdo
National Institute for Occupational Health and Safety
M/S L-3030
1095 Willowdale Road
Morgantown, W.V. 26505, USA

which consists of a silica (SiO_2) core of radius in the μm range, coated with an aluminosilicate "clay" ($nSiO_2$+ mAl_2O_3) surface layer whose thickness is a given fraction of the core radius. The history of an electron is traced through the events of elastic scattering it undergoes with the atoms of the particle. In general, there are regions of different composition along the electron's current direction of flight in the particle, and thus the distance s between two elastic collisions (and the distance to the first collision point) is sampled according to the prescription (Kalos and Whitlock 1986)

$$s = \sum_{j=1}^{l-1} s_j - \lambda_l \left(\ln r + \sum_{j=1}^{l-1} \frac{s_j}{\lambda_j} \right), \tag{1}$$

where λ_j and s_j are, respectively, the mean free path in region j and the projected distance in that region along the electron's current direction of flight; l is such that the random number r, drawn from a uniform distribution on the interval (0,1) (we used the random number generator ran2 of Press *et al.* (1992) for this purpose), satisfies the relation

$$\sum_{j=1}^{l-1} \frac{s_j}{\lambda_j} \le -\ln r < \sum_{j=1}^{l} \frac{s_j}{\lambda_j}. \tag{2}$$

The mean free paths λ_j are given by

$$\lambda_j = \frac{A_j^{\mathrm{tot}}}{N_0 \rho_j^{\mathrm{tot}} \sigma_j^{\mathrm{tot}}}, \tag{3}$$

where $A_j^{\mathrm{tot}} = \Sigma_i n_i^{(j)} A_i$ and $\sigma_j^{\mathrm{tot}} = \Sigma_i n_i^{(j)} \sigma_i$ are the total mass per mole and total elastic-scattering cross section, respectively, for region j, whose "molecules" have each n_i atoms of species i with masses per mole A_i and total elastic-scattering cross sections σ_i; N_0 is Avogadro's number, and ρ_j^{tot} is the total mass density of region j, calculated as

$$\rho_j^{\mathrm{tot}} = \left(\sum_k \frac{w_k^{(j)}}{\rho_k} \right)^{-1}, \tag{4}$$

where ρ_k is the mass density of compound k, whose mass fraction in region j is $w_k^{(j)}$. In our problem, there are only two physically different regions, namely, the surface layer and the core of the particle, but as the electron's projected line of flight can cross more than once the same physical region, different labels j in Eqs. (1) and (2) do not necessarily refer to physically different regions.

At the collision point, the atomic species i that is responsible for the elastic scattering is selected as the i for which a random number r satisfies the relation

$$\sum_{j=1}^{i-1} p_j \le r < \sum_{j=1}^{i} p_j, \tag{5}$$

where $p_j = n_j \sigma_j / \Sigma_i n_i \sigma_i$ is the probability of encountering atom j in the collision. We assume that elastic scattering is governed by a screened Rutherford differential cross section

$$\frac{d\sigma_i(\theta)}{d\Omega} = \left(\frac{Z_i \lambda\!\!\!^{-}_r^2}{2a_0} \right)^2 \frac{1}{\left(\sin^2 \frac{1}{2}\theta + \delta_i \right)^2}, \tag{6}$$

where Z_i is the atomic number of atom i, $a_0 = \hbar^2 / m_0 e^2 \approx 5.29 \times 10^{-9}$ cm is the Bohr radius, $\lambda\!\!\!^{-}_r$ is the relativistically correct reduced wavelength of an electron of kinetic energy E,

$$\lambda\!\!\!^{-}_r = \frac{\hbar}{\sqrt{2m_0 E (1 + E/2m_0c^2)}}, \tag{7}$$

and δ_i is the atomic screening parameter, parameterized as (Newbury *et al.* 1986)

$$\delta_i = 3.4 \times 10^{-3} \frac{Z_i^{2/3}}{E}, \ (E \text{ in keV}). \tag{8}$$

An advantage of the simple functional form (6) of the elastic differential cross section is that it can be integrated analytically, giving the total elastic-scattering cross section σ_i as

$$\sigma_i = 2\pi \int_0^{\pi} \frac{d\sigma_i(\theta)}{d\Omega} \sin\theta \, d\theta = \left(\frac{Z_i \lambda\!\!\!^{-}_r^2}{2a_0} \right)^2 \frac{4\pi}{\delta_i (1 + \delta_i)}, \tag{9}$$

and that the equation for the sampling of the scattering angle θ in terms of a random number r,

$$r = \frac{2\pi}{\sigma_i} \int_0^{\theta} \frac{d\sigma_i(\theta')}{d\Omega} \sin\theta' \, d\theta' \tag{10}$$

can be solved easily, giving

$$\cos\theta = 1 - \frac{2\delta_i r}{1 + \delta_i - r}. \tag{11}$$

The azimuthal angle ϕ of the scattering is assumed to be uniformly distributed on the interval (0,2π), and thus it is sampled using a random number r very simply:

$$\phi = 2\pi r, \tag{12}$$

Before the sampling of the electron's direction, the electron's kinetic energy E is adjusted for losses due to small-angle inelastic events that would occur on the path from the preceding elastic collision using the Bethe stopping-power

formula, modified for a multielement region j as (Heinrich 1981):

$$S_j = \frac{2\pi e^4 N_0 \rho_j^{\text{tot}}}{A_j^{\text{tot}} E} \sum_i n_i^{(j)} Z_i \ln \frac{\varepsilon E}{J_i}, \tag{13}$$

where ρ_j^{tot} and $A_j^{\text{tot}} = \Sigma_i n_i^{(j)} A_i$ are the same as in Eq. (3), $\varepsilon = (\frac{1}{2}e)^{1/2} \approx 1.166$, and J_i is the mean ionization potential for atom i, parameterized as (Newbury *et al.* 1986)

$$J_i = (9.76Z_i + 58.5Z_i^{-0.19}) \times 10^{-3} \quad \text{(keV)}. \tag{14}$$

For the electron's path $s = \Sigma_j d_j$ from the preceding elastic collision, where d_j is the length of the path's segment in region j, the energy is corrected as

$$E \to E - \sum_j S_j d_j. \tag{15}$$

Note that here only the length of the last segment of the path, that is, the path segment in the region in which the current collision occurs, differs from the projected distances s_j in Eqs. (1) and (2). The electron's history is terminated when the electron energy is less than the smallest critical energy for the production of x-rays of interest or when the electron escapes from the particle.

X-Ray Production

To calculate the production of the x-rays of interest, we use the Bethe cross section for inner shell ionization (Bethe 1930):

$$Q = \frac{\pi e^4 n_s b_s}{E_c^2} \frac{\ln(c_s U)}{U}, \tag{16}$$

where E_c is the critical ionization energy for a given shell and atom, the electron energy E is expressed in terms of an "overvoltage" $U = E/E_c$, n_s is the number of electrons in the shell, and b_s and c_s are constants specific to the shell. We consider only K-shell ionizations, for which we employ the values $c_K = 1$ and $b_K = 0.52+0.0029Z$ (Newbury *et al.* 1986); $n_K = 2$. The x-ray yield $N_x^{(i)}$ due to the K-shell ionization of atoms of species i along the electron's path between two successive collisions, $s = \Sigma_j d_j$, where d_j is the path's segment in region j, is calculated as

$$N_x^{(i)} = \omega_i Q_i N_0 \sum_j \frac{\rho_j^{\text{tot}} n_i^{(j)}}{A_j^{\text{tot}}} d_j \gamma_j^{(i)}, \tag{17}$$

where ω_i and Q_i are the K-shell fluorescence yield and ionization cross section (16), respectively, for atom i; $\gamma_j^{(i)}$ is an absorption factor, and the remaining symbols are as defined in the preceding subsection.

For the absorption factor $\gamma_j^{(i)}$, we use the expression

$$\gamma_j^{(i)} = \exp\left(-\sum_k \mu_k^{\text{tot}(i)} \rho_k^{\text{tot}} t_k^{(j)} \right), \tag{18}$$

where $t_k^{(j)}$ is the length of the trajectory the x-rays would have to traverse in region k on the way from the midpoint of the electron path's segment d_j to a detector placed at a given direction with respect to the incident electron beam; $\mu_k^{\text{tot}(i)}$ is the total mass absorption coefficient in region k for the x-rays produced by atom i, which is calculated in terms of the mass absorption coefficients $\mu_l^{(i)}$ of atoms l as

$$\mu_k^{\text{tot}(i)} = \sum_l w_l^{(k)} \mu_l^{(i)}, \tag{19}$$

where $w_l^{(k)}$ are the mass fractions of atoms l in region k.

The Monte Carlo estimates Y_i^{MC} of the yields of the x-rays of atoms i are obtained by accumulating the yields (17) along the whole trajectory of the electron in the particle and by summing these over all the N electron trajectories generated in a Monte Carlo simulation:

$$Y_i^{\text{MC}} = \Delta\Omega_d \sum_{n=1}^{N} \sum_m N_x^{(i)}(n,m). \tag{20}$$

Here, the indices n and m label the contributions $N_x^{(i)}$ by the trajectory and the straight segments defined by two successive collision points of a trajectory, respectively, and $\Delta\Omega_d$ is the solid angle subtended by the detector, which is assumed to be 100% efficient. Relative x-ray yields are independent of the detector solid angle $\Delta\Omega_d$ and, apart from their statistical uncertainty, of the total number N of the electron histories used.

Results and Discussion

The quantity of our interest is the relative x-ray yield

$$f_{\text{Si,Al}} = \frac{Y_{\text{Si}}}{Y_{\text{Si}} + Y_{\text{Al}}} \tag{21}$$

at a given angle Θ with respect to the direction of the incident electron beam. Here, Y_{Si} and Y_{Al} are the yields of the K_α-line x-rays of Si and Al, produced in a particle of a given geometry and composition. Our aim was to obtain the incident-electron-energy dependence of the ratio $f_{\text{Si,Al}}$, not the absolute x-ray yields Y_{Si} and Y_{Al} from any given sample.

We performed Monte Carlo calculations of the ratio $f_{\text{Si,Al}}$ for particles of several diameters in the range 0.8–3.4 μm. In quartz particles of these dimensions, the ratio $f_{\text{Si,Al}}$ has been measured at incident electron energies from 5 to 20 keV, and an aluminosilicate surface contamination reported on the basis of the one-dimensional model of Wal-

lace *et al.* (1990, 1994). In the calculations, the particles were assumed to be spherical, each with a silica (SiO_2) core of a given diameter that is coated with a clay surface layer of a given thickness. As in Wallace *et al.* (1990), the composition of clay was assumed to have equal atomic fractions of Si and Al, which is representative of typical aluminosilicates. The basic units ("molecules") of clay were thus $2SiO_2+Al_2O_3$. The thickness of the clay surface layer of a model particle of a given total diameter was fixed by requiring that the calculations adequately reproduce the ratio $f_{Si,Al}$ that has been measured on an experimentally studied particle of the same "diameter" (which was, more precisely, the particle's average width as seen in the electron microscope).

We used the tables of Heinrich (1966) and Eq. (19) to obtain the following values of the mass absorption coefficients for the Al and Si K_α-line x-rays in silica SiO_2 and clay $2SiO_2+Al_2O_3$: μ^{Al}_{silica} = 1036.7 cm^2/g, μ^{Al}_{clay} = 979.2 cm^2/g, μ^{Si}_{silica} = 668.0 cm^2/g and μ^{Si}_{clay} = 1419.5 cm^2/g. The mass density of clay was calculated using Eq. (4) with the values ρ_{silica}= 2.32 g/cm^3 and $\rho_{Al_2O_3}$= 3.97 g/cm^3 as ρ_{clay} = 2.87 g/cm^3. The values used for the critical K_α-ionization energies and fluorescence yields were E_c^{Al} = 1.56 keV, E_c^{Si} = 1.84 keV, ω_{Al} = 0.040 and ω_{Si} = 0.055 (Heinrich 1981).

Figures 1–5 present the Monte Carlo results (solid line) for particles of total diameters (clay surface thicknesses) 0.8 (0.05), 1.0 (0.06), 1.5 (0.06), 2.0 (0.12) and 3.38 (0.075) μm, respectively, compared with the experimental values of Wallace *et al.* (1990, 1994) of the ratio $f_{Si,Al}$ for quartz particles of the same "diameter." The error bars of the experimental points are due to the scatter of the several (~10) measurements that were taken at each energy. In the calculations, the incident electrons were aimed at a given particle along a line going through its center, and the electron beam profile was assumed to be very small compared with the radius of the particle. The angle of detection Θ was taken as 160° with respect to the incident electron beam, but the results were found not to be sensitive to even a relatively large variation of this angle. All these specifications were in accordance with the experimental conditions at which the experimental data were obtained. No more than 10,000 electron histories were required to be sampled at a given energy to determine the ratio $f_{Si,Al}$ to a relative statistical error smaller than 1%. The Monte Carlo calculations were performed for electron incident energies from 4 to 30 keV in steps of 0.5 keV, and the solid lines in Figures 1–5 were obtained by a smooth interpolation between these energies.

Apart from the above calculations, we also performed Monte Carlo calculations in which we assumed that each given particle had the compound Al_2O_3 distributed uniformly through its volume in such a concentration that the ratio $f_{Si,Al}$ at the high incident electron energies would coincide with that obtained when the particle was assumed to have an aluminosilicate surface layer. For a given homogeneous composition, the mass density was calculated using Eq. (4), and the x-ray mass absorption coefficients

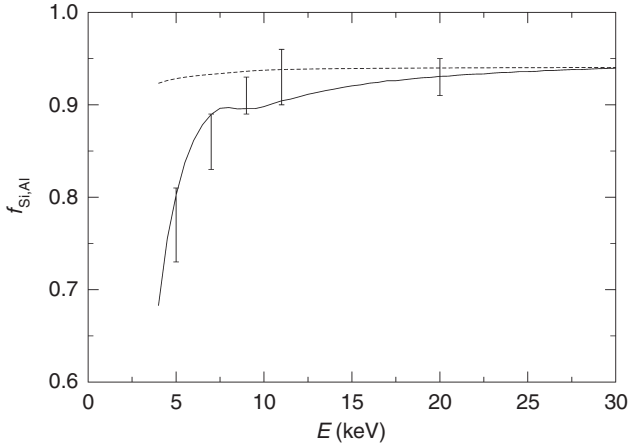

FIG. 1 The relative x-ray yield $f_{Si,Al}$ at a detection angle Θ = 160 deg versus the incident electron energy E. The full line is for a particle of a total diameter of 0.8 μm, with a 0.05 μm surface layer of clay, and the broken line is as for the full line but with Al_2O_3 distributed uniformly through the particle's volume at a concentration that reproduces the yield $f_{Si,Al}$ for the surface-layered particle at the high energies. The points with error bars are experimental data.

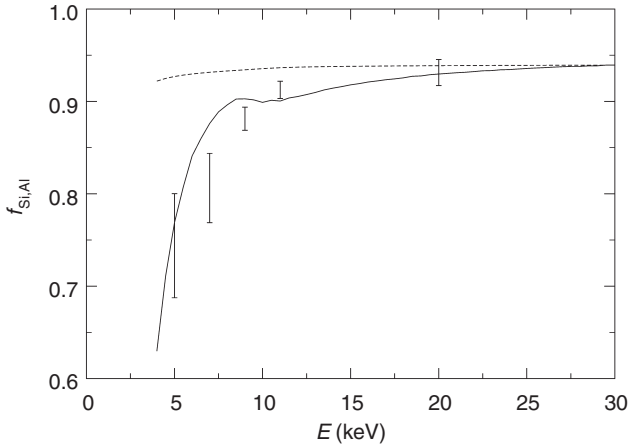

FIG. 2 As in Figure 1, but for a particle of a total diameter of 1.0 μm, covered with a 0.06 μm surface layer of clay.

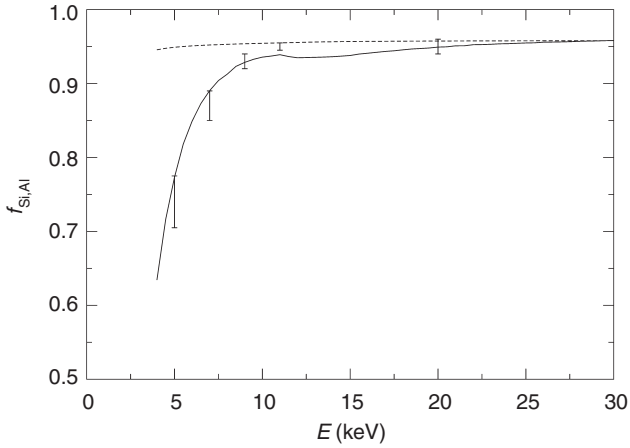

FIG. 3 As in Figure 1, but for a particle of a total diameter of 1.5 μm, covered with 0.06 μm surface layer of clay.

were obtained according to Eq. (19), in a manner similar to that for the different regions of a particle with a clay surface layer. The results of these calculations are shown in Figures 1–5 by broken lines.

It is seen in Figures 1–5 that, in view of the relatively large experimental errors (which do not include uncertainties associated with the shape and size of the particles), the Monte Carlo calculations reproduce reasonably well the measured ratio $f_{\mathrm{Si,Al}}$ and its dependence on the incident electron energy. An interesting feature of the Monte Carlo predictions for the particles of diameter $d \lesssim 2$ μm is a shallow minimum occurring just when a Monte Carlo prediction starts to level off after its steep rise at the low energies. While this feature seems to be consistent with the present experimental data, a much higher experimental accuracy would be needed to investigate it properly. We note that a similar minimum was also present in the results of Monte Carlo calculations in which the particle was schematically modeled by an infinitely extended planar silica slab of thickness equal to the diameter of the particle's silica core and with a surface aluminosilicate coating of the same thickness as that on the spherical particle.

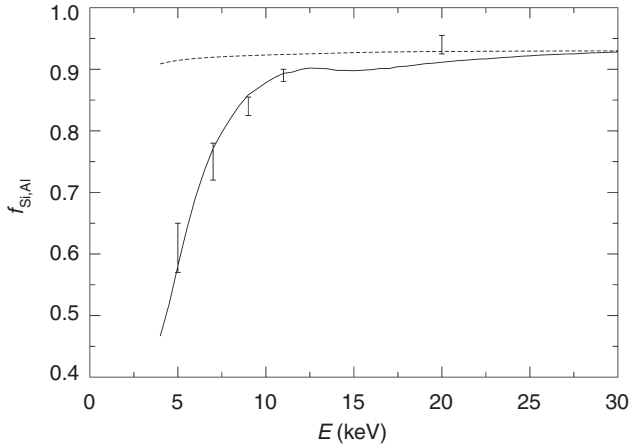

FIG. 4 As in Figure 1, but for a particle of a total diameter of 2.0 μm, covered with a 0.12 μm surface layer of clay.

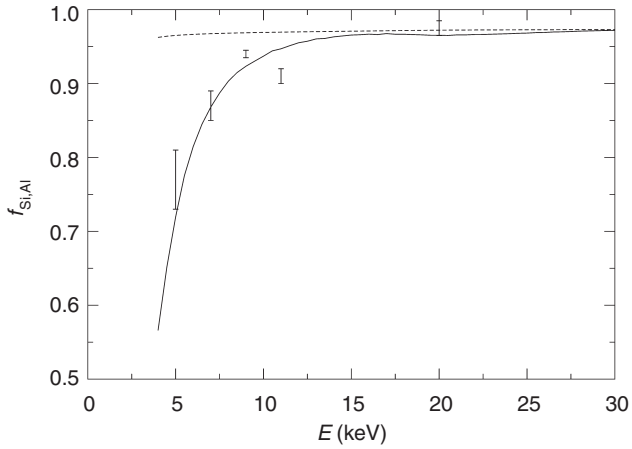

FIG. 5 As in Figure 1, but for a particle of a total diameter of 3.38 μm, covered with a 0.075 μm surface layer of clay.

The Monte Carlo calculations that assumed a homogeneous composition of the particles show almost no energy dependence, in sharp contrast to the pronounced rise in the ratio $f_{\mathrm{Si,Al}}$ at low energies obtained in the calculations that assumed that the particles had a clay surface layer. Here it should be noted that only when the composition is homogeneous is the calculated x-ray ratio $f_{\mathrm{Si,Al}}$ close to the assumed overall atomic ratio of Si to Si plus Al in the particle. When the aluminum resides in a surface layer only, the x-ray ratio $f_{\mathrm{Si,Al}}$ obtained at high energies is greater than that which would be obtained for the same particle but with all its aluminum distributed uniformly through the whole volume. A simple calculation gives the atomic ratio of Si to Si plus Al as $f^{\mathrm{atomic}}_{\mathrm{Si,Al}} = 1 - \frac{3}{2}(t/R)[1 - (t/R) + \frac{1}{3}(t/R)^2]$, where R and t are the particle's total radius and surface clay coating thickness, respectively. On the other hand, the x-ray ratio $f_{\mathrm{Si,Al}}$ for such a particle is at a sufficiently high electron energy close to $f_{\mathrm{Si,Al}} = 1 - \frac{1}{2}(t/R)$, and thus $f^{\mathrm{atomic}}_{\mathrm{Si,Al}} = 3f_{\mathrm{Si,Al}}(1 - 2f_{\mathrm{Si,Al}} + \frac{4}{3}f^2_{\mathrm{Si,Al}})$.

Several refinements of the present Monte Carlo model are possible. Instead of the time-honored formulae of Bethe for the stopping power and K-shell ionization, Eqs. (13) and (16), respectively, empirical expressions for these quantities (Casnati *et al.* 1982, Joy and Luo 1989,) that are more accurate at low electron energies can be employed. Effects such as the x-ray production by fast secondary electrons and electron backscattering from the substrate may be of some importance for absolute x-ray yields. Recently, the effect of fast secondary electrons on elemental x-ray microanalysis has been studied in detailed Monte Carlo calculations by Gauvin *et al.* (1999), with a conclusion that it is not important in relative measurements that employ known standards.

It was felt that all such refinements should not affect significantly the relative quantity $f_{\mathrm{Si,Al}}$ that was the object of our calculation. A more realistic treatment of electron elastic scattering, such as the use of tabulated Mott scattering amplitudes instead of the simple screened Rutherford differential cross section, was also not considered necessary for the same reason, especially when the deviations from the Rutherford cross section are known to be important at lower energies and at higher atomic numbers than those relevant to our study. A more complicated shape and structure of the particles can be implemented easily in a Monte Carlo calculation; more accurate and detailed experimental information than that presently available would be needed to justify such a detailed calculation.

Conclusion

The Monte Carlo model of the production of x-rays in quartz particles of respirable size validates the simple

schematic model of Wallace *et al.* (1990), on the basis of which it has been proposed that the incident electron energy dependence of the relative x-ray yield $f_{Si,Al}$ be used as a means of detection of a clay surface layer on the particles. We believe that the Monte Carlo model captures sufficiently realistically all the processes that are important for the relative quantity $f_{Si,Al}$—but if more accurate and extended experimental data would warrant it, the model can be modified easily for a still more realistic treatment and to include effects that are presently neglected. The calculations using the model show that x-ray scanning electron microscopy can be used to analyze the structure of respirable quartz particles in much more detail than just their bulk elemental composition.

Acknowledgments

The authors are grateful to Sidney Soderholm, Bill Chisholm, and Vladimir Murashov for useful comments on the manuscript.

References

Bethe HA: Zur Theorie des Durchgangs schneller Korpuskularstrahlen durch Materie. *Ann Phys (Leipzig)* 5, 322–400 (1930)

Casnati E, Tartari A, Baraldi C: An empirical approach to K-shell ionization cross section by electrons. *J Phys B* 15, 155–167 (1982)

Gauvin R, Hovington RP, Drouin D: The effect of fast secondary electrons on x-ray microanalysis in the scanning electron microscope. *Scanning* 21, 238–245 (1999)

Heinrich KFJ: X-ray absorption uncertainty. *The Electron Microprobe.* (Eds. McKinley TD, Heinrich KFJ, Wittry DB). Wiley, New York (1966) 296–377

Heinrich KFJ: *Electron Beam X-Ray Microanalysis*. Van Nostrand Reinhold, New York (1981)

Heinrich KFJ, Newbury DE, Yakowitz H (Eds.): *Use of Monte Carlo Calculations in Electron Probe Microanalysis and Scanning Electron Microscopy*. National Bureau of Standards Special Publication 460, Washington, D.C. (1976)

Joy DC: *Monte Carlo Modeling for Microscopy and Microanalysis.* Oxford University Press, Oxford (1995)

Joy DC, Luo S: An empirical stopping power relationship for low-energy electrons. *Scanning* 11, 176–180 (1989)

Kalos MH, Whitlock PA: *Monte Carlo Methods*, Volume I. Wiley, New York (1986) Sec. 6.3

LeBouffant L, Daniel H, Martin LC, Bruyere S: Effects of impurities and associated minerals on quartz toxicity. *Ann Occup Hyg* 26, 625–634 (1982)

National Institute for Occupational Safety and Health: *NIOSH recommended standard: Crystalline Silica* (DHHS-PHS-CDC-NIOSH Publication #NIOSH 75–120). U.S. Government Printing Office, Washington, D.C. (1974)

Newbury DE, Joy DC, Echlin P, Fiori CE, Goldstein JI: *Advanced Scanning Electron Microscopy and X-Ray Microanalysis*. Plenum Press, New York (1986) Chapter 1

Pouchou JL, Pichoir F: Analyse d'echatillions a la microsonde electronique. *J de Physique C2* 45, 47–50 (1984)

Press WE, Teukolsky SA, Vetterling WT, Flannery BP: *Numerical Recipes in Fortran,* 2nd ed. Cambridge University Press, Cambridge (1992)

Rokbok K, Klosterkotter W: Investigations into the specific toxicity of different SiO_2 and silica dusts *Staub Reinhart Luft* 33, 3360–63 (1973)

Wallace WE, Harrison J, Keane MJ, Bolsaitis P, Eppelsheimer D, Poston J, Page SJ: Clay occlusion of respirable quartz particles detected by low voltage scanning electron microscopy–x-ray analysis. *Ann Occup Hyg* 34, 195–204 (1990)

Wallace WE, Harrison JC, Grayson RL, Keane MJ, Bolsaitis P, Kennedy RD, Wearden AQ, Attfield MD: Aluminosilicate surface contamination of respirable quartz particles from coal mine dusts and from clay works dusts. "Inhaled Particles VII". *Ann Occup Hyg* 38, (1994) (suppl 1): 439–445